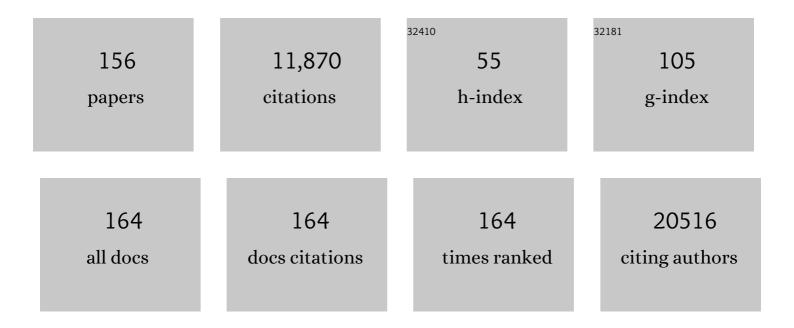
Raymond R Unocic

List of Publications by Year in descending order

Source: https://exaly.com/author-pdf/3246686/publications.pdf Version: 2024-02-01



#	Article	IF	CITATIONS
1	Selective Antisite Defect Formation in WS ₂ Monolayers via Reactive Growth on Dilute Wâ€Au Alloy Substrates. Advanced Materials, 2022, 34, e2106674.	11.1	14
2	Applications of Liquid Cell-TEM in Corrosion Research. , 2022, , 121-150.		2
3	Atomic Edge-Guided Polyethylene Crystallization on Monolayer Two-Dimensional Materials. Macromolecules, 2022, 55, 559-567.	2.2	6
4	Ammonia-Assisted Light Alkane Anti-coke Reforming on Isolated ReO _{<i>x</i>} Sites in Zeolite. ACS Catalysis, 2022, 12, 3165-3172.	5.5	6
5	In-Situ Study of Microstructure Evolution of Spinodal Decomposition in an Al-Rich High-Entropy Alloy. Frontiers in Materials, 2022, 9, .	1.2	2
6	A facile strategy for the growth of high-quality tungsten disulfide crystals mediated by oxygen-deficient oxide precursors. Nanoscale, 2022, 14, 9485-9497.	2.8	9
7	Laser-Assisted Synthesis of Monolayer 2D MoSe ₂ Crystals with Tunable Vacancy Concentrations: Implications for Gas and Biosensing. ACS Applied Nano Materials, 2022, 5, 9129-9139.	2.4	6
8	Atomic defects, functional groups and properties in MXenes. Chinese Chemical Letters, 2021, 32, 339-344.	4.8	40
9	Probing the Local Site Disorder and Distortion in Pyrochlore High-Entropy Oxides. Journal of the American Chemical Society, 2021, 143, 4193-4204.	6.6	60
10	Intrinsic Defects in MoS ₂ Grown by Pulsed Laser Deposition: From Monolayers to Bilayers. ACS Nano, 2021, 15, 2858-2868.	7.3	40
11	Reduction and Agglomeration of Supported Metal Clusters Induced by High-Flux X-ray Absorption Spectroscopy Measurements. Journal of Physical Chemistry C, 2021, 125, 11048-11057.	1.5	13
12	Unlocking the Catalytic Potential of TiO ₂ -Supported Pt Single Atoms for the Reverse Water–Gas Shift Reaction by Altering Their Chemical Environment. Jacs Au, 2021, 1, 977-986.	3.6	46
13	Designing Atomic Edge Structures in 2D Transition Metal Dichalcogenides for Improved Catalytic Activity. Microscopy and Microanalysis, 2021, 27, 964-965.	0.2	0
14	Nanoscale oxidation behavior of carbon fibers revealed with in situ gas cell STEM. Scripta Materialia, 2021, 199, 113820.	2.6	5
15	In Situ TEM Investigation of Lithium Intercalation in Ti ₃ C ₂ T _X MXenes for Energy Storage Applications. Microscopy and Microanalysis, 2021, 27, 2736-2737.	0.2	5
16	Practical Aspects of Performing Quantitive EELS Measurements of Gas Compositions in Closed-Cell Gas Reaction S/TEM. Microscopy and Microanalysis, 2021, 27, 796-798.	0.2	0
17	Atomic-scale Feedback-controlled Electron Beam Fabrication of 2D Materials. Microscopy and Microanalysis, 2021, 27, 3072-3073.	0.2	0
18	In Situ TEM Investigation of the Spontaneous Hollowing of Alloy Anode Nanocrystals. Microscopy and Microanalysis, 2021, 27, 1972-1973.	0.2	0

#	Article	IF	CITATIONS
19	Enhancing Hydrogen Evolution Activity of Monolayer Molybdenum Disulfide via a Molecular Proton Mediator. ACS Catalysis, 2021, 11, 12159-12169.	5.5	19
20	Dynamic restructuring of supported metal nanoparticles and its implications for structure insensitive catalysis. Nature Communications, 2021, 12, 7096.	5.8	33
21	Nickel particle–enabled width-controlled growth of bilayer molybdenum disulfide nanoribbons. Science Advances, 2021, 7, eabk1892.	4.7	19
22	Investigating local oxidation processes in Fe thin films in a water vapor environment by in situ liquid cell TEM. Ultramicroscopy, 2020, 209, 112842.	0.8	11
23	Statistical learning of governing equations of dynamics from in-situ electron microscopy imaging data. Materials and Design, 2020, 195, 108973.	3.3	8
24	Broadening the Gas Separation Utility of Monolayer Nanoporous Graphene Membranes by an Ionic Liquid Gating. Nano Letters, 2020, 20, 7995-8000.	4.5	39
25	Cadmium Selective Etching in CdTe Solar Cells Produces Detrimental Narrow-Gap Te in Grain Boundaries. ACS Applied Energy Materials, 2020, 3, 1749-1758.	2.5	6
26	<i>In situ</i> electrochemical scanning/transmission electron microscopy of electrode–electrolyte interfaces. MRS Bulletin, 2020, 45, 738-745.	1.7	19
27	Fluid-Guided CVD Growth for Large-Scale Monolayer Two-Dimensional Materials. ACS Applied Materials & Interfaces, 2020, 12, 26342-26349.	4.0	14
28	Spontaneous and reversible hollowing of alloy anode nanocrystals for stable battery cycling. Nature Nanotechnology, 2020, 15, 475-481.	15.6	68
29	Effect of lattice mismatch and shell thickness on strain in core@shell nanocrystals. Nanoscale Advances, 2020, 2, 1105-1114.	2.2	45
30	Pt-Ligand single-atom catalysts: tuning activity by oxide support defect density. Catalysis Science and Technology, 2020, 10, 3353-3365.	2.1	28
31	Surfactant-Mediated Growth and Patterning of Atomically Thin Transition Metal Dichalcogenides. ACS Nano, 2020, 14, 6570-6581.	7.3	30
32	Lattice Strain Measurement of Core@Shell Electrocatalysts with 4D Scanning Transmission Electron Microscopy Nanobeam Electron Diffraction. ACS Catalysis, 2020, 10, 5529-5541.	5.5	39
33	Predicting synthesizable multi-functional edge reconstructions in two-dimensional transition metal dichalcogenides. Npj Computational Materials, 2020, 6, .	3.5	23
34	Disorder-to-Order Transition Mediated by Size Refocusing: A Route toward Monodisperse Intermetallic Nanoparticles. Nano Letters, 2019, 19, 6418-6423.	4.5	26
35	Superior electrocatalytic hydrogen evolution at engineered non-stoichiometric two-dimensional transition metal dichalcogenide edges. Journal of Materials Chemistry A, 2019, 7, 18357-18364.	5.2	30
36	Building Random Alloy Surfaces from Intermetallic Seeds: A General Route to Strain-Engineered Electrocatalysts with High Durability. ACS Applied Nano Materials, 2019, 2, 4538-4546.	2.4	15

#	Article	IF	CITATIONS
37	Effect of Synthesis Methods on the Structure and Defects of Two-Dimensional MXenes. , 2019, , 111-123.		1
38	Multi-modal characterization approach to understand proton transport mechanisms in solid oxide fuel cells. Microscopy and Microanalysis, 2019, 25, 2048-2049.	0.2	0
39	Synthesis of Ni-Rich Thin-Film Cathode as Model System for Lithium Ion Batteries. ACS Applied Energy Materials, 2019, 2, 1405-1412.	2.5	31
40	lsotope-Engineering the Thermal Conductivity of Two-Dimensional MoS ₂ . ACS Nano, 2019, 13, 2481-2489.	7.3	42
41	Mechanochemical Synthesis of High Entropy Oxide Materials under Ambient Conditions: Dispersion of Catalysts via Entropy Maximization. , 2019, 1, 83-88.		143
42	Atom-by-atom fabrication with electron beams. Nature Reviews Materials, 2019, 4, 497-507.	23.3	73
43	Atomic Insight into Thermolysisâ€Driven Growth of 2D MoS ₂ . Advanced Functional Materials, 2019, 29, 1902149.	7.8	28
44	Defect-Mediated Phase Transformation in Anisotropic Two-Dimensional PdSe ₂ Crystals for Seamless Electrical Contacts. Journal of the American Chemical Society, 2019, 141, 8928-8936.	6.6	81
45	Interpreting Electrochemical and Chemical Sodiation Mechanisms and Kinetics in Tin Antimony Battery Anodes Using <i>in Situ</i> Transmission Electron Microscopy and Computational Methods. ACS Applied Energy Materials, 2019, 2, 3578-3586.	2.5	14
46	Current Density Distribution in Electrochemical Cells with Small Cell Heights and Coplanar Thin Electrodes as Used in ec-S/TEM Cell Geometries. Journal of the Electrochemical Society, 2019, 166, H126-H134.	1.3	20
47	Achieving Highly Durable Random Alloy Nanocatalysts through Intermetallic Cores. ACS Nano, 2019, 13, 4008-4017.	7.3	37
48	Decoding crystallography from high-resolution electron imaging and diffraction datasets with deep learning. Science Advances, 2019, 5, eaaw1949.	4.7	81
49	Nanoscale mapping of the electron density at Al grain boundaries and correlation with grain-boundary energy. Physical Review Materials, 2019, 3, .	0.9	4
50	Mechanochemicalâ€Assisted Synthesis of Highâ€Entropy Metal Nitride via a Soft Urea Strategy. Advanced Materials, 2018, 30, e1707512.	11.1	325
51	Multi-purposed Ar gas cluster ion beam processing for graphene engineering. Carbon, 2018, 131, 142-148.	5.4	18
52	Influence of Nonstoichiometry on Proton Conductivity in Thin-Film Yttrium-Doped Barium Zirconate. ACS Applied Materials & Interfaces, 2018, 10, 4816-4823.	4.0	18
53	Atomically Dispersed Co and Cu on N-Doped Carbon for Reactions Involving C–H Activation. ACS Catalysis, 2018, 8, 3875-3884.	5.5	63
54	Evolutionary selection growth of two-dimensional materials on polycrystalline substrates. Nature Materials, 2018, 17, 318-322.	13.3	204

#	Article	IF	CITATIONS
55	Predictive multiphase evolution in Al-containing high-entropy alloys. Nature Communications, 2018, 9, 4520.	5.8	107
56	In situ edge engineering in two-dimensional transition metal dichalcogenides. Nature Communications, 2018, 9, 2051.	5.8	100
57	The Influence of Local Distortions on Proton Mobility in Acceptor Doped Perovskites. Chemistry of Materials, 2018, 30, 4919-4925.	3.2	40
58	Reduction of Propionic Acid over a Pd-Promoted ReO _{<i>x</i>} /SiO ₂ Catalyst Probed by X-ray Absorption Spectroscopy and Transient Kinetic Analysis. ACS Sustainable Chemistry and Engineering, 2018, 6, 12353-12366.	3.2	14
59	Pioneering the Use of Neural Network Architectures and Feature Engineering for Real-Time Augmented Microscopy and Analysis. Microscopy and Microanalysis, 2018, 24, 514-515.	0.2	0
60	In situ atomistic insight into the growth mechanisms of single layer 2D transition metal carbides. Nature Communications, 2018, 9, 2266.	5.8	125
61	Avoiding Fracture in a Conversion Battery Material through Reaction with Larger Ions. Joule, 2018, 2, 1783-1799.	11.7	65
62	NiAl Oxidation Reaction Processes Studied In Situ Using MEMS-Based Closed-Cell Gas Reaction Transmission Electron Microscopy. Oxidation of Metals, 2017, 88, 495-508.	1.0	17
63	Precision controlled atomic resolution scanning transmission electron microscopy using spiral scan pathways. Scientific Reports, 2017, 7, 43585.	1.6	23
64	Distinct nanoscale reaction pathways in a sulfide material for sodium and lithium batteries. Journal of Materials Chemistry A, 2017, 5, 11701-11709.	5.2	51
65	Facet-Dependent Deposition of Highly Strained Alloyed Shells on Intermetallic Nanoparticles for Enhanced Electrocatalysis. Nano Letters, 2017, 17, 5526-5532.	4.5	92
66	Building with ions: towards direct write of platinum nanostructures using in situ liquid cell helium ion microscopy. Nanoscale, 2017, 9, 12949-12956.	2.8	8
67	Competitive Ion Diffusion within Grain Boundary and Grain Interiors in Polycrystalline Electrodes with the Inclusion of Stress Field. Journal of the Electrochemical Society, 2017, 164, A2830-A2839.	1.3	11
68	Deep Learning of Atomically Resolved Scanning Transmission Electron Microscopy Images: Chemical Identification and Tracking Local Transformations. ACS Nano, 2017, 11, 12742-12752.	7.3	282
69	Anisotropic Etching of Hexagonal Boron Nitride and Graphene: Question of Edge Terminations. Nano Letters, 2017, 17, 7306-7314.	4.5	54
70	A Discovery of Strong Metal–Support Bonding in Nanoengineered Au–Fe ₃ O ₄ Dumbbell-like Nanoparticles by in Situ Transmission Electron Microscopy. Nano Letters, 2017, 17, 4576-4582.	4.5	27
71	Suppression of Defects and Deep Levels Using Isoelectronic Tungsten Substitution in Monolayer MoSe ₂ . Advanced Functional Materials, 2017, 27, 1603850.	7.8	84
72	A Novel Electrolyte Salt Additive for Lithiumâ€lon Batteries with Voltages Greater than 4.7 V. Advanced Energy Materials, 2017, 7, 1601397.	10.2	103

#	Article	IF	CITATIONS
73	Selective Aerobic Oxidation of Alcohols over Atomicallyâ€Dispersed Nonâ€Precious Metal Catalysts. ChemSusChem, 2017, 10, 359-362.	3.6	79
74	In situ Nanoscale Imaging and Spectroscopy of Energy Storage Materials. Microscopy and Microanalysis, 2017, 23, 1964-1965.	0.2	0
75	An Atomistic Carbide-Derived Carbon Model Generated Using ReaxFF-Based Quenched Molecular Dynamics. Journal of Carbon Research, 2017, 3, 32.	1.4	13
76	Impact of Membraneâ€Induced Particle Immobilization on Seeded Growth Monitored by In Situ Liquid Scanning Transmission Electron Microscopy. Small, 2016, 12, 2701-2706.	5.2	18
77	Building with Ions: Development of In-situ Liquid Cell Microscopy for the Helium Ion Microscope Microscopy and Microanalysis, 2016, 22, 754-755.	0.2	Ο
78	Inverse Problem Solution for Quantitative Investigations of Nanocrystals Formation and Growth. Microscopy and Microanalysis, 2016, 22, 794-795.	0.2	0
79	Directing Matter: Toward Atomic-Scale 3D Nanofabrication. ACS Nano, 2016, 10, 5600-5618.	7.3	99
80	Size-Dependent Disorder–Order Transformation in the Synthesis of Monodisperse Intermetallic PdCu Nanocatalysts. ACS Nano, 2016, 10, 6345-6353.	7.3	185
81	Creep deformation mechanism mapping in nickel base disk superalloys. Materials at High Temperatures, 2016, 33, 372-383.	0.5	74
82	Atomic Defects in Monolayer Titanium Carbide (Ti ₃ C ₂ T _{<i>x</i>}) MXene. ACS Nano, 2016, 10, 9193-9200.	7.3	785
83	Direct-write liquid phase transformations with a scanning transmission electron microscope. Nanoscale, 2016, 8, 15581-15588.	2.8	29
84	Atomistic-Scale Simulations of Defect Formation in Graphene under Noble Gas Ion Irradiation. ACS Nano, 2016, 10, 8376-8384.	7.3	113
85	Influence of Dioxygen on the Promotional Effect of Bi during Pt-Catalyzed Oxidation of 1,6-Hexanediol. ACS Catalysis, 2016, 6, 4206-4217.	5.5	21
86	The Effect of Carbonate and pH on Hydrogen Oxidation and Oxygen Reduction on Pt-Based Electrocatalysts in Alkaline Media. Journal of the Electrochemical Society, 2016, 163, F291-F295.	1.3	11
87	Patterning: Atomic‣evel Sculpting of Crystalline Oxides: Toward Bulk Nanofabrication with Single Atomic Plane Precision (Small 44/2015). Small, 2015, 11, 5854-5854.	5.2	2
88	In situ Electrochemical TEM for Quantitative Nanoscale Imaging Dynamics of Solid Electrolyte Interphase and Lithium Electrodeposition. Microscopy and Microanalysis, 2015, 21, 2437-2438.	0.2	2
89	Lowâ€Temperature CO Oxidation over a Ternary Oxide Catalyst with High Resistance to Hydrocarbon Inhibition. Angewandte Chemie, 2015, 127, 13461-13465.	1.6	8
90	Atomicâ€Level Sculpting of Crystalline Oxides: Toward Bulk Nanofabrication with Single Atomic Plane Precision. Small, 2015, 11, 5895-5900.	5.2	73

#	Article	IF	CITATIONS
91	Lowâ€Temperature CO Oxidation over a Ternary Oxide Catalyst with High Resistance to Hydrocarbon Inhibition. Angewandte Chemie - International Edition, 2015, 54, 13263-13267.	7.2	87
92	In situ Liquid S/TEM: Practical Aspects, Challenges, and Opportunities. Microscopy and Microanalysis, 2015, 21, 2295-2296.	0.2	0
93	Ruthenium-Alloy Electrocatalysts with Tunable Hydrogen Oxidation Kinetics in Alkaline Electrolyte. Journal of Physical Chemistry C, 2015, 119, 13481-13487.	1.5	104
94	Vapor Synthesis and Thermal Modification of Supportless Platinum–Ruthenium Nanotubes and Application as Methanol Electrooxidation Catalysts. ACS Applied Materials & Interfaces, 2015, 7, 10115-10124.	4.0	16
95	Ruthenium as a CO-tolerant hydrogen oxidation catalyst for solid acid fuel cells. Journal of Materials Chemistry A, 2015, 3, 3984-3987.	5.2	15
96	The Effect of Carbonate and pH on Hydrogen Oxidation and Oxygen Reduction on Pt-Based Electrocatalysts in Alkaline Media. ECS Transactions, 2015, 69, 995-1005.	0.3	0
97	Synthesis of Hexagonal Boron Nitride Monolayer: Control of Nucleation and Crystal Morphology. Chemistry of Materials, 2015, 27, 8041-8047.	3.2	202
98	Nanoscale Imaging of Fundamental Li Battery Chemistry: Solid-Electrolyte Interphase Formation and Preferential Growth of Lithium Metal Nanoclusters. Nano Letters, 2015, 15, 2011-2018.	4.5	185
99	Supportless, Bismuth-Modified Palladium Nanotubes with Improved Activity and Stability for Formic Acid Oxidation. ACS Catalysis, 2015, 5, 5154-5163.	5.5	34
100	Large-scale delamination of multi-layers transition metal carbides and carbonitrides "MXenes― Dalton Transactions, 2015, 44, 9353-9358.	1.6	662
101	Aqueous proton transfer across single-layer graphene. Nature Communications, 2015, 6, 6539.	5.8	214
102	Water desalination using nanoporous single-layer graphene. Nature Nanotechnology, 2015, 10, 459-464.	15.6	1,372
103	Quantitative Description of Crystal Nucleation and Growth from in Situ Liquid Scanning Transmission Electron Microscopy. ACS Nano, 2015, 9, 11784-11791.	7.3	41
104	Platinum and Palladium Overlayers Dramatically Enhance the Activity of Ruthenium Nanotubes for Alkaline Hydrogen Oxidation. ACS Catalysis, 2015, 5, 7015-7023.	5.5	44
105	Probing battery chemistry with liquid cell electron energy loss spectroscopy. Chemical Communications, 2015, 51, 16377-16380.	2.2	25
106	Direct Visualization of Solid Electrolyte Interphase Formation in Lithium-Ion Batteries with <i>In Situ</i> Electrochemical Transmission Electron Microscopy. Microscopy and Microanalysis, 2014, 20, 1029-1037.	0.2	83
107	Quantitative Electrochemical Measurements Using <i>In Situ</i> ec-S/TEM Devices. Microscopy and Microanalysis, 2014, 20, 452-461.	0.2	80
108	<i>In-Situ</i> Electrochemical Transmission Electron Microscopy for Battery Research. Microscopy and Microanalysis, 2014, 20, 484-492.	0.2	45

#	Article	IF	CITATIONS
109	Direct visualization of initial SEI morphology and growth kinetics during lithium deposition by in situ electrochemical transmission electron microscopy. Chemical Communications, 2014, 50, 2104.	2.2	172
110	High performance Cr, N-codoped mesoporous TiO ₂ microspheres for lithium-ion batteries. Journal of Materials Chemistry A, 2014, 2, 1818-1824.	5.2	58
111	Bis(fluoromalonato)borate (BFMB) anion based ionic liquid as an additive for lithium-ion battery electrolytes. Journal of Materials Chemistry A, 2014, 2, 7606-7614.	5.2	31
112	Direct measurement of the chemical reactivity of silicon electrodes with LiPF6-based battery electrolytes. Chemical Communications, 2014, 50, 3081.	2.2	56
113	Unraveling manganese dissolution/deposition mechanisms on the negative electrode in lithium ion batteries. Physical Chemistry Chemical Physics, 2014, 16, 10398.	1.3	59
114	Probing the Mechanism of Sodium Ion Insertion into Copper Antimony Cu ₂ Sb Anodes. Journal of Physical Chemistry C, 2014, 118, 7856-7864.	1.5	64
115	Formation of a Metallic Amorphous Layer During the Sliding Wear of Ti/TiN Nanolaminates. Tribology Letters, 2014, 55, 219-226.	1.2	3
116	Role of Surface Functionality in the Electrochemical Performance of Silicon Nanowire Anodes for Rechargeable Lithium Batteries. ACS Applied Materials & Interfaces, 2014, 6, 7607-7614.	4.0	30
117	Sodium Manganese Oxide Thin Films as Cathodes for Na-Ion Batteries. ECS Transactions, 2014, 58, 47-57.	0.3	10
118	Tuning Electrodeposition Parameters for Tailored Nanoparticle Size, Shape, and Morphology: An In Situ ec-STEM Investigation. Microscopy and Microanalysis, 2014, 20, 1506-1507.	0.2	1
119	In operando Transmission Electron Microscopy Imaging of SEI Formation and Structure in Li-Ion and Li-Metal Batteries. Microscopy and Microanalysis, 2014, 20, 1538-1539.	0.2	1
120	Novel Method for Precision Controlled Heating of TEM Thin Sections to Study Reaction Processes. Microscopy and Microanalysis, 2014, 20, 1628-1629.	0.2	1
121	Mo3Sb7 as a very fast anode material for lithium-ion and sodium-ion batteries. Journal of Materials Chemistry A, 2013, 1, 11163.	5.2	121
122	Defect chemistry of phospho-olivine nanoparticles synthesized by a microwave-assisted solvothermal process. Journal of Solid State Chemistry, 2013, 205, 197-204.	1.4	8
123	Demonstration of an Electrochemical Liquid Cell for Operando Transmission Electron Microscopy Observation of the Lithiation/Delithiation Behavior of Si Nanowire Battery Anodes. Nano Letters, 2013, 13, 6106-6112.	4.5	265
124	Gas evolution from cathode materials: A pathway to solvent decomposition concomitant to SEI formation. Journal of Power Sources, 2013, 239, 341-346.	4.0	34
125	Characterization of sodium ion electrochemical reaction with tin anodes: Experiment and theory. Journal of Power Sources, 2013, 234, 48-59.	4.0	186
126	Mesoporous TiO2 spheres with a nitridated conducting layer for lithium-ion batteries. Journal of Materials Science, 2013, 48, 5125-5131.	1.7	18

#	Article	IF	CITATIONS
127	Solid electrolyte coated high voltage layered–layered lithium-rich composite cathode: Li1.2Mn0.525Ni0.175Co0.1O2. Journal of Materials Chemistry A, 2013, 1, 5587.	5.2	137
128	Coupling EELS/EFTEM Imaging with Environmental Fluid Cell Microscopy. Microscopy and Microanalysis, 2012, 18, 1104-1105.	0.2	2
129	In-situ liquid and gas transmission electron microscopy of nano-scale materials. Microscopy and Microanalysis, 2012, 18, 1158-1159.	0.2	8
130	Conductive surface modification of LiFePO4 with nitrogen-doped carbon layers for lithium-ion batteries. Journal of Materials Chemistry, 2012, 22, 4611.	6.7	76
131	High cyclability of ionic liquid-produced TiO2 nanotube arrays as an anode material for lithium-ion batteries. Journal of Power Sources, 2012, 218, 88-92.	4.0	50
132	A Topotactic Synthetic Methodology for Highly Fluorineâ€Doped Mesoporous Metal Oxides. Angewandte Chemie - International Edition, 2012, 51, 2888-2893.	7.2	13
133	Influence of Periodic Nitrogen Functionality on the Selective Oxidation of Alcohols. Chemistry - an Asian Journal, 2012, 7, 387-393.	1.7	57
134	Fabrication and characterization of Li–Mn–Ni–O sputtered thin film high voltage cathodes for Li-ion batteries. Journal of Power Sources, 2012, 211, 108-118.	4.0	71
135	Fabrication and design aspects of high-temperature compact diffusion bonded heat exchangers. Nuclear Engineering and Design, 2012, 249, 49-56.	0.8	100
136	Dislocation decorrelation and relationship to deformation microtwins during creep of a γ′ precipitate strengthened Ni-based superalloy. Acta Materialia, 2011, 59, 7325-7339.	3.8	150
137	Mesoporous TiO ₂ –B Microspheres with Superior Rate Performance for Lithium Ion Batteries. Advanced Materials, 2011, 23, 3450-3454.	11.1	361
138	Dopamine as a Carbon Source: The Controlled Synthesis of Hollow Carbon Spheres and Yolkâ€ S tructured Carbon Nanocomposites. Angewandte Chemie - International Edition, 2011, 50, 6799-6802.	7.2	674
139	TEM and In-situ Liquid Cell Characterization of Copper Nanowire Growth Mechanisms. Microscopy and Microanalysis, 2011, 17, 462-463.	0.2	0
140	<i>In-situ</i> TEM Characterization of Electrochemical Processes in Energy Storage Systems. Microscopy and Microanalysis, 2011, 17, 1564-1565.	0.2	13
141	Characterization of Pre- and Post-Service Grain Boundary Phases in a Cast Austenitic Steel. , 2011, , .		0
142	The Importance of High-Resolution Scanning Transmission Electron Microscopy For Fine-Scale Dislocation Analysis. Microscopy and Microanalysis, 2010, 16, 1798-1799.	0.2	0
143	Characterization of Metamorphic GaAsP/Si Materials and Devices for Photovoltaic Applications. IEEE Transactions on Electron Devices, 2010, 57, 3361-3369.	1.6	99
144	Low cycle fatigue of a Ni-based superalloy: Non-planar deformation. Scripta Materialia, 2010, 62, 790-793.	2.6	34

#	Article	IF	CITATIONS
145	Direct exfoliation of natural graphite into micrometre size few layers graphene sheets using ionic liquids. Chemical Communications, 2010, 46, 4487.	2.2	295
146	The intermediate temperature deformation of Ni-based superalloys: Importance of reordering. Jom, 2009, 61, 42-48.	0.9	41
147	Microtwinning and other shearing mechanisms at intermediate temperatures in Ni-based superalloys. Progress in Materials Science, 2009, 54, 839-873.	16.0	305
148	HAADF Imaging and MD Simulations of Microtwining Partial Dislocations in Nickel Based Superalloy Rene 104,. Microscopy and Microanalysis, 2008, 14, 938-939.	0.2	0
149	Microtwinning during intermediate temperature creep of polycrystalline Ni-based superalloys: mechanisms and modelling. Philosophical Magazine, 2006, 86, 4823-4840.	0.7	57
150	The Creep Deformation Mechanisms of Nickel Base Superalloy Ren \tilde{A} © 104. Microscopy and Microanalysis, 2005, 11, .	0.2	2
151	Merging Biological Self-Assembly with Synthetic Chemical Tailoring: The Potential for 3-D Genetically Engineered Micro/Nano-Devices (3-D GEMS). International Journal of Applied Ceramic Technology, 2005, 2, 317-326.	1.1	67
152	Process efficiency measurements in the laser engineered net shaping process. Metallurgical and Materials Transactions B: Process Metallurgy and Materials Processing Science, 2004, 35, 143-152.	1.0	112
153	Anatase assemblies from algae: coupling biological self-assembly of 3-D nanoparticle structures with synthetic reaction chemistry. Chemical Communications, 2004, , 796.	2.2	67
154	Composition control in the direct laser-deposition process. Metallurgical and Materials Transactions B: Process Metallurgy and Materials Processing Science, 2003, 34, 439-445.	1.0	20
155	Application of Electrochemical Liquid Cells for Electrical Energy Storage and Conversion Studies. , 0, , 237-257.		1
156	Nanoscale Oxidation Behavior of Carbon Fibers Revealed with <i>in situ</i> Gas Cell STEM. SSRN Electronic Journal, 0, , .	0.4	0